Check for updates

Advanced Engineering Materials

ADVANCED ENGINEERING MATERIALS
www.aem-journal.com

RESEARCH ARTICLE OPEN ACCESS

Optimization of the Production of Rubber Compounds Using Mathematical Models

Anke Bardehle[1] | Andreas Limper[1] | Ulrich Giese[2] | Carlos Lucke[2] | Mario Beiner[3] | Christoph Gögelein[4] | Lisa Leuchtenberger-Engel[1] | Christian Hopmann[1]

[1]Institute for plastics processing (IKV), RWTH Aachen, Aachen, Germany | [2]Deutsches Institut für Kautschuktechnologie, Hannover, Germany | [3]Fraunhofer Institute for Microstructure of Materials and Systems, Halle, Germany | [4]ARLANXEO Deutschland GmbH, Dormagen, Germany

Correspondence: Anke Bardehle (publications@ikv.rwth-aachen.de)

Received: 24 December 2025 | **Revised:** 2 April 2026 | **Accepted:** 13 April 2026

Keywords: mathematical models | optimization | rubber compounding

ABSTRACT

Rubber compounds are produced in a discontinuously working internal mixer with the addition of components such as rubber, fillers, plasticizers, and chemicals. In order to ensure a high quality, mixing instructions must be developed for each recipe. Optimal process settings are currently determined iteratively based on expert knowledge. As the scale-up from lab to production machines is not possible today, these process developments take place on production machines, which is limited in terms of time, costs, and material. Therefore, the aim is to predict and subsequently optimize the mixing process depending on the recipe and process parameters. In order to develop initial approaches for describing the entire mixing process, mathematical models are being developed using symbolic regression to describe the ram path and torque as well as the mixing quality based on incorporation, dispersion, and distribution. Overall, sufficient accuracy can be achieved for predicting the ram path and torque. The following optimization using evolutionary algorithms enables a reduction in energy input up to 40%.

1 | Introduction

Producing rubber compounds is the first step in production of high-quality elastomer products like seals. Rubber compounds are almost exclusively mixed in discontinuously working internal mixers. This offers, for example, the advantages of high flexibility and the ability to accept a variety of different dosing forms (bales, powder, oil, etc.) [1]. In order to produce rubber compounds, recipes consisting of, for example, polymer, fillers, and the curing system are produced according to specified mixing instructions.

Both the development of the recipe and the associated mixing instructions are currently determined and optimized iteratively, based primarily on expert knowledge [2]. In the mixing process, specified requirements such as the break-up of filler agglomerates and the homogenization of the components have to be ensured. Insufficiently dispersed fillers can cause defects in the end product, resulting in a reduction of product properties such as abrasion [1]. Furthermore, the current iterative development of mixing instructions results in difficulties when integrating new raw materials and technological innovations into the development of rubber products.

To address these issues, developments towards data digitization and the prediction of the mixing process based on process and material models are promising in order to accelerate the finding of suitable mixing instructions. Since it is currently not possible to describe the entire mixing process based on models, the focus of this paper is primarily on modeling individual mixing phases, which then can be combined into a higher-level model and optimized in terms of mixing time and energy afterwards. Challenges include the complex rheological properties of rubber compounds, the partial filling of the mixing chamber, and the changing material properties during the mixing process [3]. In order to develop initial approaches for describing the entire mixing process and thus determine the process and material parameters being relevant for the individual mixing phases, mathematical models are

This is an open access article under the terms of the Creative Commons Attribution License, which permits use, distribution and reproduction in any medium, provided the original work is properly cited.

© 2026 The Author(s). *Advanced Engineering Materials* published by Wiley-VCH GmbH.

created using symbolic regression (SR). For the investigation of material parameters, only the influence of different Ethylene-Propylen-Dien-Rubber (EPDM) types is examined in order to identify whether it is possible to integrate material parameters into the prediction of mixing processes. As models developed by SR are used to optimize the mixing process regarding mixing time and energy input, evolutionary algorithms are used to determine the optimum mixing time and energy input. Since the focus is on optimizing the mixing time and energy input rather than on compliance with end product specifications, it is not taken into account that the use of different polymers leads to different end product properties.

2 | State-of-the-Art

The following chapter discusses the principles of rubber compound production as well as methods for modeling rubber compound production.

2.1 | Production of Rubber Compounds

During compound mixing, requirements such as the homogenization and dispersion of components and the compliance with certain temperature limits are specified [4]. In order to describe different mixing tasks, the mixing process is divided into phases. A rough subdivision can be made into the masterbatch and final mixing processes [1]. The production of the masterbatch includes the incorporation of different fillers such as carbon black and chalk and plasticizers into the polymer matrix, whereas in the final mixing process the vulcanization system is distributed [1]. Concerning the masterbatch mixing process, carbon black agglomerates, which are formed during carbon black production, have to be dispersed. The shear and elongation forces required for this are applied by the rotors rotating against each other in the mixing chamber and by drag of material through the gap between the mixing chamber and the rotors.

Besides the dispersion, a homogeneous distribution of the components in the mixture is required [1]. Depending on the polymer used, the masterbatch mixing process is performed as a conventional or an upside- down mixing process. In a conventional mixing process, the polymer is first added to the mixing chamber and mixed for a specified time [4]. The fillers are added afterwards. For synthetic rubbers such as EPDM with a high filler content, the upside-down mixing process has proven to be effective, where the fillers, plasticizers, and additives are added to the mixing chamber before the rubber [1]. This means that the mixer is already completely filled at the start of the mixing process, allowing higher shear forces to be introduced into the mixture [4]. An example of a mixing curve for an upside-down basic mixing process using EPDM and carbon black is shown in Figure 1.

The mixing curve represents the development of process variables over time, such as the ram path and the power input. As the mixing curves are recorded for each mixing process, a direct correlation between the measured variables and the selected process parameters can be derived. These mixing curves can be used to analyze and optimize mixing parameters for the individual mixing phases [2, 5, 6]. To ensure a suitable incorporation of the fillers, the masterbatch mixing process is divided into the phases incorporation and dispersion and homogenization. In the incorporation phase, the fillers and plasticizers are added to the mixing chamber. This is directly followed by the addition of the polymer. When the ram is lowered, the filler incorporation phase is initiated, and a first power peak occurs (A). This is caused by the increase of fill factor in the mixing chamber [7]. During carbon black incorporation, the increase in compound temperature leads to a reduction in compound viscosity and thus to a lower power input [4]. Simultaneously, due to filler incorporation, the filler content in the mixture increases and thus the viscosity, which results in a second power maximum (B) [4]. In order to determine the end of the incorporation phase, the ram path is used [5]. It decreases to its final position as incorporation continues. The duration until the end of incorporation is referred to as the black incorporation time (BIT). The lowering of the ram can be used to evaluate the fill factor. With an optimal fill factor, the ram reaches its final position with a time delay and then oscillates around this position [2]. An immediate lowering indicates underfilling, whereas a longer

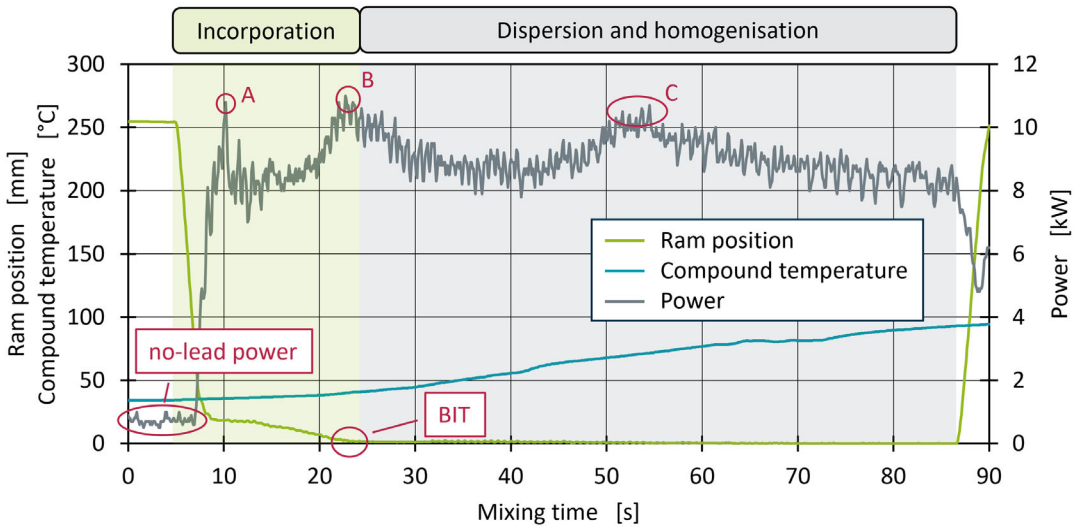


FIGURE 1 | Mixing curve for an upside-down mixing process.

15272648, 0, Downloaded from https://advanced.onlinelibrary.wiley.com/doi/10.1002/adem.202503201 by Universitatsbibliothek RWTH Aachen University, Wiley Online Library on [29/05/2026]. See the Terms and Conditions (https://onlinelibrary.wiley.com/terms-and-conditions) on Wiley Online Library for rules of use; OA articles are governed by the applicable Creative Commons License

ram lowering time indicates overfilling [2]. Following this phase, the carbon black dispersion and compound homogenization starts. During the dispersion phase, in certain cases a further power peak can be observed (C) correlating with the dispersion of carbon black [8].

2.2 | Modeling of Rubber Mixing Processes

The modeling of the mixing process is the subject of numerous research works [2, 9, 10]. For example, it was shown that the use of neural networks predicts the elastic torque measured in rotational rheometry for an solution styrene-butadiene rubber silica compound with a description accuracy of 89% [10]. Another research work deals with the description of the compound viscosity during mixing. To predict the compound viscosity online, neural networks were used [9]. In order to predict the incorporation time depending on process parameters and the type of carbon black used, modeling approaches using neural networks were carried out at the Institute for Plastics Processing (IKV). However, in this case, only a coefficient of determination of less than 0.48 could be achieved [11].

An alternative for predicting the mixing process based on neural networks is the determination of mathematical models. In order to predict the filler incorporation phase, mathematical equations were determined in a previous study using genetic algorithms, indicating the dependence of the ram position and the torque on the process parameters, for example, fill factor and rotor speed, as well as carbon black content as material parameter [12]. This resulted in an average deviation between the calculated and measured values of less than 10% for the incorporation time and less than 2% for the torque, which complied with the specified maximum deviation of 15% [12]. Based on these models describing the incorporation phase, physically inspired correlations were integrated in a subsequent study [8]. The influences of the drag volume flow, polymer type, and carbon black content on the ram position and the development of filler incorporation were investigated [8]. At present, a complete modeling of the mixing process is only possible with highly simplified boundary conditions, such as the assumption of a completely filled mixing chamber [13, 14].

For this reason, the following hypotheses will be examined in in this study

1. Mathematical models describing the ram position and the torque during the mixing process can be developed using evolutionary algorithms. These models can describe the development of the mixing curves as well as the development of the mixing process (incorporation, dispersion, and distribution) depending on the mixing time.
2. The models developed can be used to determine the process parameters and polymer type which result in optimized energy input and mixing time.

2.2.1 | Genetic and Evolutionary Algorithm

Genetic and evolutionary algorithms are describing methods which are used to solve complex optimization problems based on strategies of evolutionary biology under appropriate boundary conditions [15]. Each step of the optimization is referred to a generation, which consists of a specified number of individuals with particular results. The individuals are summarized under the term population. After each generation, the individuals of a population are evaluated. A new generation is then selected using the strategies of selection, recombination and mutation [15]. In the field of compound mixing, the evolutionary optimization strategy has already been applied in the final mixing process to predict the rotor speed in order to reduce mixing time and energy input [16].

2.2.1.1 | Symbolic Regression. To determine mathematical equations which are supposed to be calculated based on data points, the SR can be applied. SR is a data-driven method based on genetic programing, which is inspired by biological evolution and is widely used to produce arithmetic expressions for modeling learning tasks [17]. In the case of SR, an individual of a generation corresponds to a model equation consisting of a sequence of operators (e.g. subtraction, multiplication, summation) and a dataset of real measurements [18]. Compared to other statistical methods, the SR results are given by an arbitrary set of mathematical operators that represent arbitrarily complex linear and nonlinear functions without a predefined fixed structure. Therefore, in contrast to other machine learning algorithms, this method provides interpretable results [17].

3 | Experimental Design

In order to develop models describing the mixing curves and the mixing quality depending on EPDM- polymer type and process parameters (e.g. rotor speed, temperature control) using SR, a dataset based on experimental data is prepared. The basic recipe selected for this purpose, using EPDM rubber, carbon black and a sulfur vulcanization system is shown in Table 1.

TABLE 1 | Mixing recipe.

Component	Brand name	Manufacturer	Amount, phr
Polymer	EPDM	Arlanxeo Deutschland GmbH, Dormagen	100.0
Carbon black	N550	Cabot GmbH, Rheinfelden	65.0
Vulcanization activator	Zinc oxide active	Lanxess Deutschland GmbH, Cologne	5.0
Vulcanization activator	Stearic acid	Emery Oelochemicals GmbH, Düsseldorf	1.0
Curing agent	Sulfur 90—95	Solvay & Barium Strontium GmbH & Co. KG, Hannover	1.5
Curing aid	Rhenogran CBS-80	Lanxess Deutschland GmbH, Cologne	3.5
Curing aid	Rhenogran MBT-80	Lanxess Deutschland GmbH, Cologne	1.0

15272648, 0, Downloaded from https://advanced.onlinelibrary.wiley.com/doi/10.1002/adem.202503201 by Universitatsbibliothek RWTH Aachen University, Wiley Online Library on [29/05/2026]. See the Terms and Conditions (https://onlinelibrary.wiley.com/terms-and-conditions) on Wiley Online Library for rules of use; OA articles are governed by the applicable Creative Commons License

All experimental investigations were carried out with an internal mixer of type GK 1.5E (Harburg-Freudenberger Maschinenbau GmbH, Freudenberg) with the intermeshing rotor geometry PES5. All compounds were produced using an upside-down mixing process where carbon black, the curing activators and the curing agent and aids were added to the mixing chamber before the polymer.

To analyze the influence of polymer properties on the mixing process, seven EPDM polymer types were selected, which differ in their average molecular weight, molecular weight distribution, and ethylene content (Table 2). A method developed by Arlanxeo is used to provide a qualitative parameter which enables the comparison of the molecular weight and molecular weight distribution of different polymers.

For this purpose, frequency sweep tests were carried out using the RPA Ultra, which exposes an oscillating stress on the compound [19, 20]. The force to be exerted follows the displacement with a phase shift. The measured shear modulus (G*) can be subdivided into the storage modulus (G') and the loss modulus (G") using the phase angle (δ). Purely elastic systems have a phase angle of 0° and purely viscous systems 90° [21]. To predict the average molecular weight, δ is considered. At a high angular frequency of 10^2 rad/s, this is almost completely determined by the average molecular weight [22]. An increase in δ indicates a reduction in the average molecular weight. The molecular weight distribution is determined using the parameter Δδ as a parameter for the nonNewtonian viscoelastic behavior of EPDM polymers due to the long-chain branching and the corresponding broadening of the molecular weight distribution [22]. For EPDM Δδ is calculated by subtracting δ at the frequency of 10^2 rad/s from the phase angle of the frequency of 10^{-1} rad/s at a temperature of 125°C [22]. An increase in Δδ indicates an increase in the molecular weight distribution. The results for δ, Δδ and ethylene content are listed in Table 2.

All polymer types are characterized by a density of 0.86 g/cm* and are not extended with oil. Expect for the polymer Keltan 4460D all polymer types have an ethylene content of less than 55 wt.-% and are therefore classified as amorphous EPDM polymers [23]. The polymer Keltan 4460D contains a higher ethylene content of about 58 wt%, which classifies it as semi-crystalline. Crystalline EPDM types with an ethylene content of more than 65 wt.-% exhibit improved flow properties compared to amorphous EPDM types [23].

The series of experiments conducted to enable prediction of the mixing curves was carried out predominantly with the EPDM grade Keltan 6950C. In these experiments, the process parameters rotor speed, rotor and mixing chamber temperature, and fill factor were systematically varied. To assess the influence of temperature control on additional polymers, trials were performed with the grades Keltan 2750 and Keltan 9950C, in which the temperature settings were also varied. This allows the influence of temperature control on molecular weight to be evaluated for comparable molecular weight distributions and ethylene contents.

To achieve a high product quality, a sufficiently high mixing quality is required. This includes complete incorporation and dispersion of the fillers and homogenization (distribution) of all components. For this purpose, the ram is first moved to its end position, which corresponds to a hight of 1.5 mm for the inter- nal mixer used. The compound is then mixed for a predefined time. To predict the mixing quality at the reference point, experiments are carried out using EPDM grade Keltan 6950C with a fill factor of 70%, a rotor speed of 45 min^{-1}, and rotor and mixing chamber temperatures of 40°C. After the respective mixing time, samples are taken and the content of incorporated and dispersed carbon black is determined.

The corresponding analytical methods are described in Chapter 3.1. For all other combinations of polymer and process parameters, only mixtures with mixing times of 10 and 30 s after the ram has reached its end position are produced. These experiments provide a basis for adjusting the curves used to describe the mixing quality. To determine the mixing behavior over longer mixing times, additional mix- tures are produces for all polymers with a fill factor of 70%, a rotor speed of 45 min^{-1}, rotor and mixing chamber temperatures of 40°C, and a mixing time of 300 s after the ram has reached its end position. In total, 52 compounds result from these experiments, which are used for model development.

An overview of all the mixing processes carried out can be taken from Table 3.

TABLE 2 | EPDM polymer types.

EPDM-polymer-type	δ, rad/s	Δδ, rad/s	Ethylene conent, wt.-%
Keltan 2750	23.8	20	48
Keltan 4450S	21.7	23	52
Keltan 4460D	21.1	13	58
Keltan 6950D	17.5	23	44
Keltan 8550C	17.1	25	48
Keltan 9650C	16.6	37	51
Keltan 9950C	15.5	22	44

3.1 | Analysis Methods

The following chapter describes the methods used to analyze the mixing curves as well as the incorporation and dispersion of the filler.

3.1.1 | Mixing Curve

For the evaluation and thus the prediction of mixing processes, mixing curves are used, which show the development of power, ram position, and rotor speed over time [6].

Both the mixing time and energy consumption are analyzed. To describe the mixing time, the ram path is taken into account, as the complete material remains in the mixing chamber after the ram has been lowered to its end position. In addition, the time required for the ram to reach its end position is used as a dimension for evaluating the fill factor. As already described, a reduced ram lowering time indicates underfilling of the mixing chamber, which leads to lower shear stress in the mixture and thus results in insufficient break-up of the filler agglomerates. In contrast, a longer ram lowering time indicates overfilling of the mixing chamber, which inhibits the homogeneous distribution of the mixture components. To evaluate the energy consumption, the

15272648, 0, Downloaded from https://advanced.onlinelibrary.wiley.com/doi/10.1002/adem.202503201 by Universitatsbibliothek RWTH Aachen University, Wiley Online Library on [29/05/2026]. See the Terms and Conditions (https://onlinelibrary.wiley.com/terms-and-conditions) on Wiley Online Library for rules of use; OA articles are governed by the applicable Creative Commons License

TABLE 3 | Overview of the mixing processes carried out.

Polymer	Fill factor, %	rotor speed, min^{-1}	TCU rotor, °C	TCU mixing chamber,°C	Mixing time after ram down, s
Keltan 6950C	70	45	40	40	0/10/20/30/40/300
Keltan 6950C	70	20	40	40	0/10/30
Keltan 6950C	70	60	40	40	0/10/30
Keltan 6950C	70	45	30	30	10/30
Keltan 6950C	70	45	80	80	10/30
Keltan 6950C	70	45	30	80	10/30
Keltan 6950C	70	45	80	30	10/30
Keltan 6950C	60	45	40	40	10/30
Keltan 6950C	65	45	40	40	10/30
Keltan 6950C	75	45	40	40	10/30
Keltan 2750	70	45	40	40	10/30/300
Keltan 2750	70	45	30	30	10/30
Keltan 2750	70	45	80	80	10/30
Keltan 9950C	70	45	40	40	10/30/300
Keltan 9950C	70	45	30	30	10/30
Keltan 9950C	70	45	80	80	10/30
Keltan 4450S	70	45	40	40	10/30/300
Keltan 4460D	70	45	40	40	10/30/300
Keltan 8550C	70	45	40	40	10/30/300
Keltan 9650C	70	45	40	40	10/30/300

torque is taken into account and can be directly determined from the mixing curve.

3.1.2 | Amount of Unincorporated Carbon Black

The amount of unincorporated carbon black is determined by using a sieve to remove the excess carbon black after discharging the compound out of the mixing chamber and determining the weight of the compound. As a result, the amount of incorporated carbon black is the difference between the amount of carbon black added and removed. It is assumed that the amount of carbon black added corresponds to the amount calculated on the basis of the recipe and the fill factor of the used internal mixer.

3.1.3 | Surface Topography

The filler dispersion is analyzed using the W 820 R roughness instrument with the TKU 400 stylus system and a resolution of 0.1 µm from Jenoptik AG, Jena. The test specimen used is cut from a 6 mm high pressed sheet using a single-edged stainless steel razor blade. For the subsequent measurement, a square area with a side length of 1 mm is measured. In total, 6 samples are measured, each with 201 lines and 1000 points. From the resulting surface, depressions and elevations, which are caused by filler agglomerates, can be detected. Insufficient dispersion is present when the absolute value of a peak exceeds 1.5 µm [24]. The area as well as the height of the individual peaks are used to evaluate the dispersion. The degree of dispersion is calculated using the area of undispersed filler agglomerates divided by the measured surface.

In the present work, mixing quality is evaluated at the compound based on dispersion and distribution metrics derived from the surface topography of the cured material. These metrics directly quantify the degree of filler dispersion and the homogeneity of the compound, which are known to correlate with the mechanical performance of vulcanized rubber (e.g. through their influence on stiffness, strength, and fatigue behavior) [1]. It should be noted that no additional mechanical testing or microscopic investigations were carried out in this study.The goal is to develop a process-oriented optimization approach and a method for quality assessment that can be applied in industrial compounding plants, where routine quality control is typically limited to Mooney viscosity and simple dispersion tests (e.g. Dispertester), and advanced microscopic analyses are rarely available. The surface-topography-based dispersion metric used here represents a more sensitive and less operator-dependent assessment of dispersion than conventional dispersion testers, while remaining closer to what can realistically be implemented in practice.

4 | Development of Mathematical Models for the Mixing Process

To optimize the mixing process in regard to mixing time and energy input, mathematical models are derived, which are able to predict the mixing quality as well as the mixing curves for the ram path and torque. In terms of mixing quality, incorporation, dispersion, and distribution are taken into account. To

15272648, 0, Downloaded from https://advanced.onlinelibrary.wiley.com/doi/10.1002/adem.202503201 by Universitatsbibliothek RWTH Aachen University, Wiley Online Library on [29/05/2026]. See the Terms and Conditions (https://onlinelibrary.wiley.com/terms-and-conditions) on Wiley Online Library for rules of use; OA articles are governed by the applicable Creative Commons License

develop the models, functions are determined for all mixing curves using SR.

This is followed by the determination of similarities between the functions, from which the superior function for the incorporation phase is derived. The identified superior functions consist, for example, of parameters depending on the process and polymer parameters (ethylene content (E), δ, Δδ, fill factor (FF), rotor speed (n), mixing chamber temperature (T_m), rotor temperature (T_R)). SR is used to describe this relation. In order to validate the established correlations using SR, the average deviation between the parameters resulting from the mixing curves or the measured data for the mixing qualities and the calculated parameters is determined. The aim is to achieve a maximum deviation of up to 15%.

Due to the limited dataset of 52 measurement points, an additional division into training and test data was specifically avoided. A fixed holdout test would have further reduced the amount of data available for model identification and, particularly in a 7-dimensional feature space, would have led to excessive parameter variability. Instead, the focus was placed on explicitly limiting model complexity and on external validation of the model. For SR, a limited function library was used. The maximum expression depth and the number of terms were restricted to avoid overly complex models. From the candidate models proposed by the symbolic regression, the equation was selected in each case that, with minimal complexity, allowed only a marginal further improvement in the performance measures. To validate the models, after optimization with respect to mixing time and energy input, a mixture was produced using optimized recipe and process parameters. This mixture was not part of the previously established data set.

4.1 | Ram Position

In order to enable subsequent calculations of the torque up to the end position of the ram and to provide an estimation of the selected fill factor of the mixing chamber, a model for the ram position as a function of the mixing time is developed. The required superior function has already been developed and validated for the fill factor and rotor speed in a previous study [12]. A function describing the dependence of the parameters on the material and process parameters has not yet been determined. As the first few seconds of the mixing process depend on the rotor position and the polymer bale size, for example, the equations are established starting at a mixing time of 10 s after reaching a height of 100 mm above the end position of the ram [12]. The resulting function for the ram path (S) depending on the mixing time (t) can be taken from Equation (1).

$$S = a - b * t \tag{1}$$

SR was used to describe parameters a and b as functions of the EPDM polymer type and the process parameters used. The resulting equations for calculating a and b are displayed below (Equations (2), (3) and (4)).

$$a = ((E - 40.96)/(\delta - \Delta\delta) + 17.98 * (FF * (1.49 + 0.18/(FF(+T_r - 106.74))) - 78.6)/\Delta\delta \tag{2}$$

$$b = (((-86.37/(E + (0.055/(b_2 - 0.8))))) + 2)/b_2) + b_2 \tag{3}$$

$$b_2 = ((-0.56/T_R) + (FG * 0.000487)) * n \tag{4}$$

A dependence of parameter a on the material parameters (ethylene content, δ, and Δδ) as well as on the process parameters (fill factor and rotor temperature) was determined. Parameter b can be described based on the ethylene content, fill factor, rotor temperature and rotor speed. In order to validate the calculated parameters, Figure 1 displays the values for the parameters a and b, which are determined using the mixing curve, as well as the calculated values. In the case of complete correlation between the values, these would be located on the blue bisector shown in the diagram Figure 2.

In addition, the average percentage deviation between the data points is calculated. This results in a deviation of less than 9% for parameter a and 10% for parameter b. To ensure sufficient accuracy, it was defined that a deviation of 15% should not be exceeded. Overall, the models developed for calculating parameters a and b of the ram path therefore achieve a sufficiently high level of accuracy.

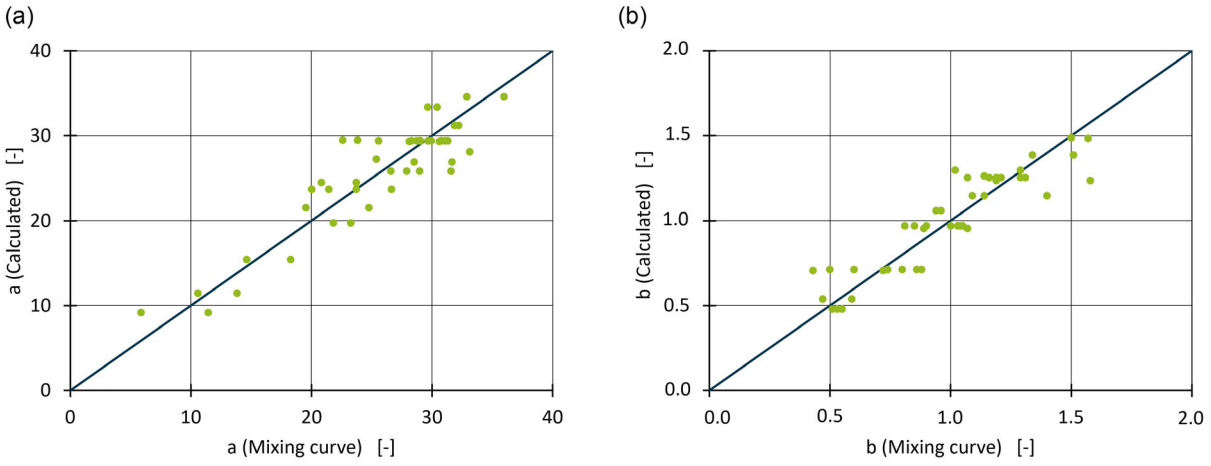


FIGURE 2 | Comparison of the parameters a and b for the torque in the first mixing phase based on the mixing curves and the calculated parameters.

15272648, 0, Downloaded from https://advanced.onlinelibrary.wiley.com/doi/10.1002/adem.202503201 by Universitatsbibliothek RWTH Aachen University, Wiley Online Library on [29/05/2026]. See the Terms and Conditions (https://onlinelibrary.wiley.com/terms-and-conditions) on Wiley Online Library for rules of use; OA articles are governed by the applicable Creative Commons License

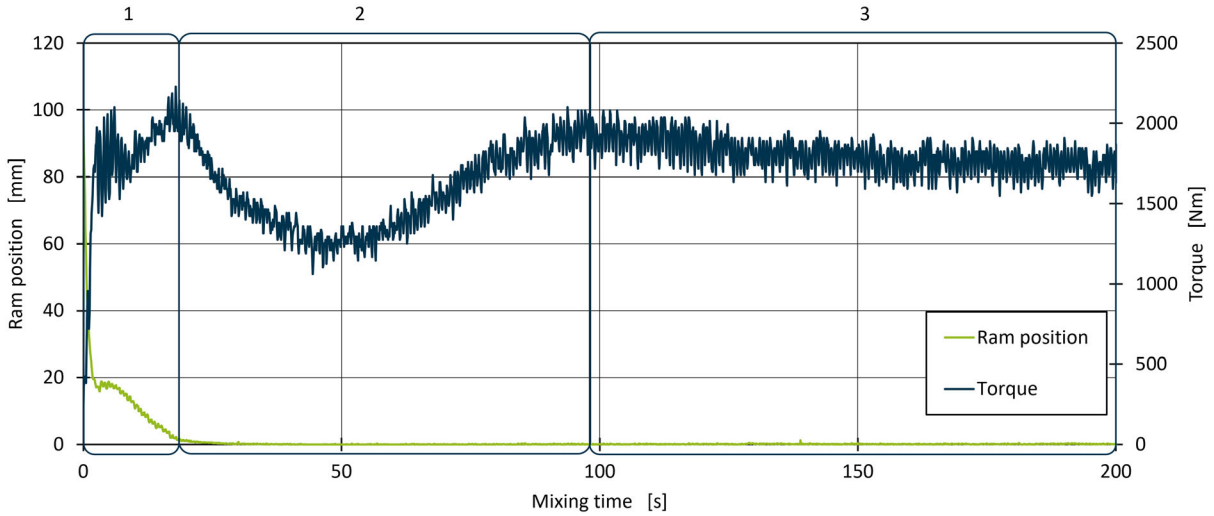


FIGURE 3 | Separation of the mixing curve into three mixing phases.

4.2 | Torque

For the optimization of energy consumption in mixing processes, models are developed describing the torque curve over the mixing time. For this purpose, the mixing process is first divided into three phases, with a separate model being developed for each phase. The division of the mixing process is illustrated in Figure 3.

The first section is characterized by the lowering of the ram towards its end position, the second section represents the area between the torque maxima, and the third section is characterized by a decrease in torque until reaching a plateau [25]. The development of the superior models and the calculation of the necessary parameters depending on the material and process parameters will be explained in the following.

4.3 | First Mixing Phase

Analogous to the superior equation for the ram path, a model was developed and validated in the previous study that provides a description of the torque curve up to the final ram position [12]. The data points from a mixing time starting at 10 s after reaching the ram position of 100 mm are included. The superior function for the torque (T_1) as a function of the ram position (S) can be obtained from Equation (5).

$$T_1 = c - d * S^2 \tag{5}$$

The parameters c and d based on the polymer and process parameters can be taken from Equations (6) and (7).

$$c = ((-4724.67/(FF - 54.99)) + 2374.86 - (\delta * (58.58 - E))) + 234.45 \tag{6}$$

$$d = (3.71/(E - (\Delta\delta * 2.2))) + ((12.27/(FF - 62.2)) + 0.59) \tag{7}$$

The dependence of the parameters c and d on the material and process parameters is determined using SR. Both parameters show a relation to the ethylene content and the fill factor. In addition, δ is included in the calculation of parameter c and Δδ in the calculation of parameter d. To validate the calculated parameters, Figure 4 shows the comparison between the parameters obtained from the mixing process and the calculated parameters.

In total, an average percentage deviation between the measured and calculated data points of 4% for parameter c and of 21% for

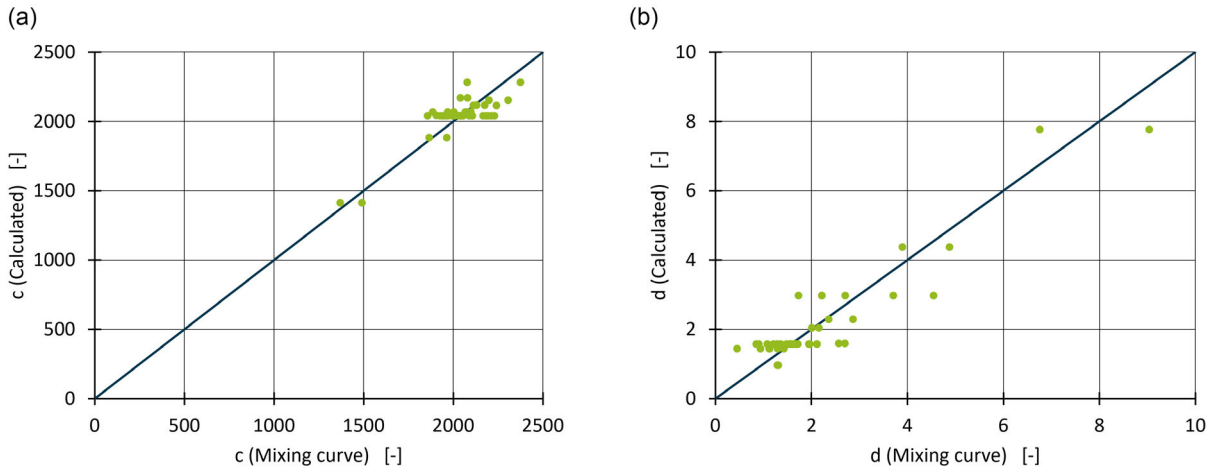


FIGURE 4 | Comparison of the parameters c and d for the torque in the first mixing phase based on the mixing curves and the calculated parameters.

15272648, 0, Downloaded from https://advanced.onlinelibrary.wiley.com/doi/10.1002/adem.202503201 by Universitatsbibliothek RWTH Aachen University, Wiley Online Library on [29/05/2026]. See the Terms and Conditions (https://onlinelibrary.wiley.com/terms-and-conditions) on Wiley Online Library for rules of use; OA articles are governed by the applicable Creative Commons License

parameter d is achieved. The deviation between the values calculated using the mixing curve and the SR exceeds the required deviation of 15%. However, further increasing the complexity of the equation determined by SR does not improve the accuracy of the prediction. One possible reason is that the mixing phase is characterized by a continuous change in material composition due to the progression of incorporation. In addition, the rubber bales are manually precut and fed into the mixing chamber, resulting in different initial conditions between runs (e.g. bale size, feeding pattern, and timing of addition). Under these conditions, parameter d can only serve as an approximate descriptor of the early mixing behavior, and a more accurate description could not be achieved with the available data. Since the parameters c and d are expressed as functions of recipe and process parameters and are subsequently used in Equation (5) below, the uncertainty of d is transferred to the subsequent predictions. This error propagation reduces the quantitative accuracy of the calculated torque curve for the first mixing phase. Nevertheless, the identified correlations capture the prevailing trends and the qualitative influence of the operating conditions and are therefore used for subsequent optimization.

4.4 | Second Mixing Phase

The second phase describing the torque is characterized by the two torque maxima. The superordinate function determined for the second phase of the torque (T_2) depending on the total rotations of the rotor (R) can be obtained from Equation (8).

$$T_2 = e * R^2 - f * R + 2000 \tag{8}$$

The parameters e and f are determined as a function of the material parameters δ, Δδ and the ethylene content (Equation (9) and (10)).

$$e = (((\delta/E) * 184.24) - E)/(\Delta\delta - 7.91) \tag{9}$$

$$f = (\delta * 149.47)/E \tag{10}$$

The validation for the two parameters can be obtained in Figure 5.

The highest average percentage deviation between the parameters obtained from the mixing curve and the calculated values is achieved for parameter e with a value of 13%. Parameter f reaches a deviation of 7%. Overall, the maximum deviation of 15% is not exceeded.

4.5 | Third Mixing Phase

During the last mixing phase, a reduction in torque is observed. This correlates with an increase in the compound temperature and a corresponding reduction in compound viscosity. All recipe components are incorporated at the beginning of this mixing phase. To provide a relation between the torque (T_3) in this mixing phase and the rotor revolutions (R), a superordinate function is defined, which can be taken from the Equation (11).

$$T_3 = g/(R + h) + i \tag{11}$$

To identify the relation between the varied parameters and the parameters g, h and i SR is applied. The resulting Equations are shown below (Equation (12), (13) and (14)).

$$g = (E * 99.76) * ((E - \Delta\delta)/((\Delta\delta + \delta) + (\delta - 53.11))) \tag{12}$$

$$h = (((E + (\Delta\delta/(\delta - 15.31))) - \Delta\delta) * 5.14) - 147.38 \tag{13}$$

$$i = (-2538.33/(\Delta\delta - 10.27)) + 1784.44 \tag{14}$$

Similar to the second mixing phase, a dependency of the parameters g and h on the material parameters δ, Δδ, and ethylene content can be determined. Parameter i indicates a dependency on Δδ only. The validation of the determined SR-models in comparison to the parameters from the mixing curves can be obtained from the Figure 6.

The average percentage deviation of the calculated parameters and the parameters obtained from the mixing curves results in a deviation of 8% for parameter g, 4% for parameter h, and 9% for parameter i. As none of the parameters exceed the required deviation of 15%, the parameters can be considered to be sufficiently accurate and are therefore included in the overall model.

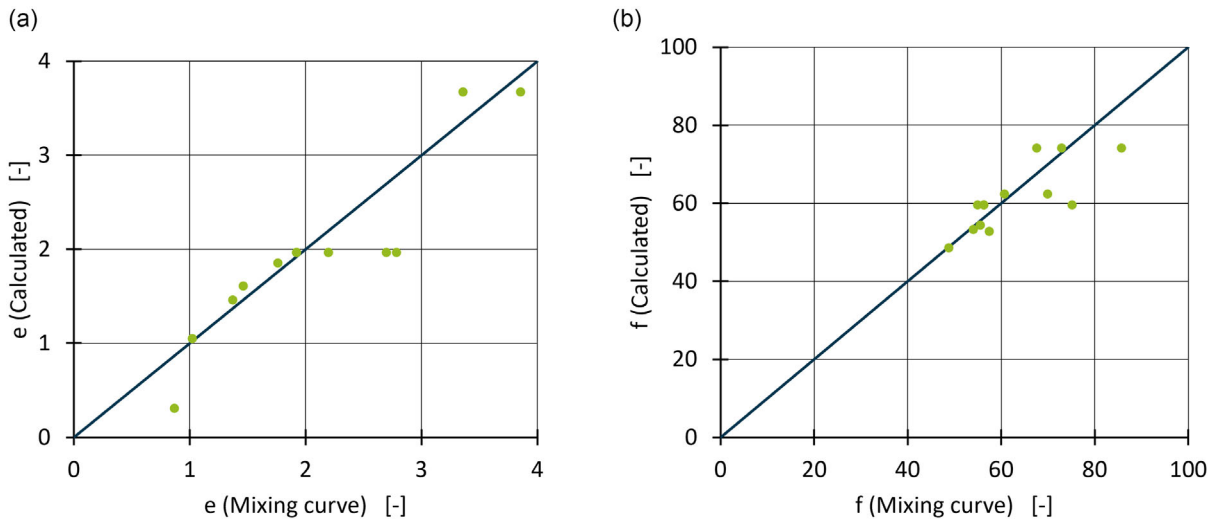


FIGURE 5 | Comparison of the parameters e and f for the torque in the first mixing phase based on the mixing curves and the calculated parameters.

15272648, 0, Downloaded from https://advanced.onlinelibrary.wiley.com/doi/10.1002/adem.202503201 by Universitatsbibliothek RWTH Aachen University, Wiley Online Library on [29/05/2026]. See the Terms and Conditions (https://onlinelibrary.wiley.com/terms-and-conditions) on Wiley Online Library for rules of use; OA articles are governed by the applicable Creative Commons License

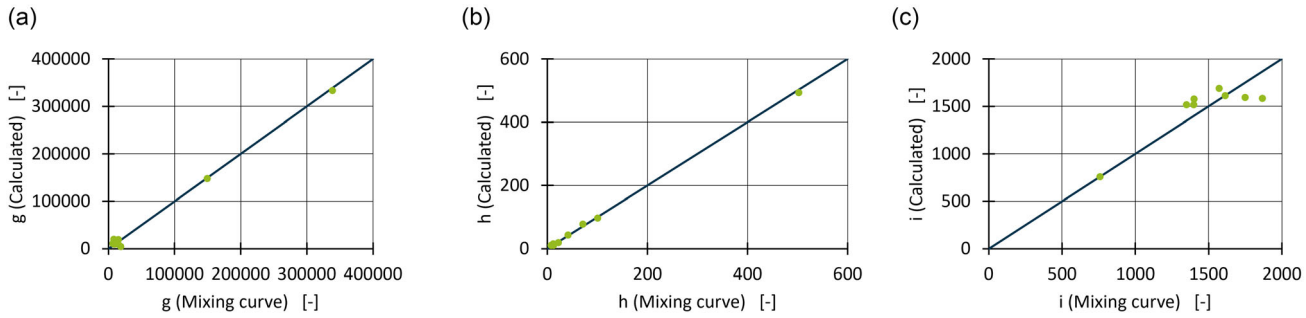


FIGURE 6 | Comparison of the parameters g, h, and i for the torque in the first mixing phase based on the mixing curves and the calculated parameters.

5 | Mixing Quality

To achieve sufficient compound quality during optimization, the mixing time has to be adjusted to ensure the fillers are fully incorporated, dispersed, and distributed homogeneously. For this reason, three models describing these three effects are developed below.

5.1 | Incorporation

Using different mixing times, compounds are produced to visualize the incorporation process. To determine the unincorporated carbon black content, the unincorporated carbon black is removed using a sieve, as described in Chapter 3. Here, incorporation is defined as the amount of incorporated carbon black compared to the amount of carbon black added. A value of 100% would therefore correspond to complete incorporation. In a previous study, a superordinate function depending on the mixing time was already determined and validated for two EPDM-polymers and 2 carbon black contents (Equation (15)) [12]. A function describing the dependence of the parameters on the material and process parameters has not yet been determined.

$$Incorporation = j - k/t \tag{15}$$

To identify the relation between the varied parameters and the parameters j and k SR is applied. The resulting Equations are shown below (Equation (16) and (17)).

$$j = (\Delta\delta * (-0.48823/(FF - 8.2448 - E))) + 1.9979 \tag{16}$$

$$k = ((FF/E) * 43.704) - n \tag{17}$$

The parameters j and k were determined using SR for all recipe and process parameter variations (Table 2 and 3). A dependency of parameter j on the material parameters Δδ and ethylene content as well as on the fill factor was determined. The parameter k shows a dependence on the fill factor and δ. The comparison of the parameters j and k, which were calculated using the measured data and the function calculated using SR, is presented in the Figure 7. In addition, the measured incorporation is shown in comparison to the calculated incorporation, which results from the parameters calculated using SR.

The average deviation for parameter *j* is 23% for parameter *k*, and 22% for the resulting incorporation. Thus, both the parameters and the total incorporation exceed the required maximum deviation of 15%. However, if only incorporation above 80% is taken into account, an average deviation of 11% can be achieved. Since an incorporation of at least 95% must be achieved for the mixing process to be completed, the model is sufficient for prediction. One possible reason for the poor prediction in the lower incorporation region could be explained by the fact that the polymer used is EPDM, which is in the form of crumbs in the mixing chamber at the start of the mixing process. As a result, it is possible that polymer was also removed during sieving, leading to the assumption of a lower incorporation than actually achieved.

5.2 | Dispersion

To determine the development of dispersion, compounds are produced according to the method used to establish the incorporation process. Afterwards, the degree of dispersion is calculated using the methodology described in the Chapter 3

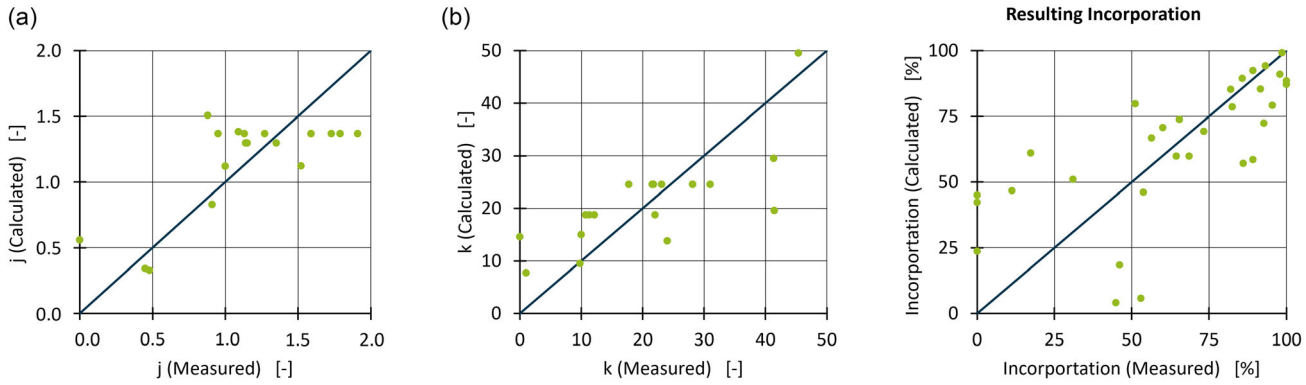


FIGURE 7 | Comparison of the parameters j and k for the torque in the first mixing phase based on the mixing curves and the calculated parameters.

15272648, 0, Downloaded from https://advanced.onlinelibrary.wiley.com/doi/10.1002/adem.202503201 by Universitatsbibliothek RWTH Aachen University, Wiley Online Library on [29/05/2026]. See the Terms and Conditions (https://onlinelibrary.wiley.com/terms-and-conditions) on Wiley Online Library for rules of use; OA articles are governed by the applicable Creative Commons License

using surface topography. In this case, dispersion is defined as the area of undispersed carbon black agglomerates in relation to the measured sample surface area. Consequently, a value of 100% would correspond to complete dispersion. The correlation for describing the dispersion depending on the mixing time (t) and parameters l and m identified by SR can be taken from the Equation (18).

$$Dispersion = l * t^{m} \tag{18}$$

The Equations (19) and (20) are showing the dependency of l and m on the polymer and process parameters.

$$l = n * (((((n + \delta/(FF - T_R)) + 33.25)/E) * 0.48493 - 0.69968)/(\Delta\delta - 17.106) - 0.07346) + 3.797 \tag{19}$$

$$m = ((-177.74/n)/\Delta\delta) + (E * 0.025484) \tag{20}$$

Using SR, a dependence of parameter l on the material parameters (ethylene content, δ, and Δδ) as well as on the process parameters (fill factor, rotor temperature, and rotor speed) was determined. Parameter m can be described based on Δδ, ethylene content and rotor speed. In order to validate the calculated parameters, Figure 8 displays the values for the parameters l, m and the resulting dispersion, which were determined using the mixing curve, as well as the calculated values.

In total an average percentage deviation between the measured and calculated data points of 14% for parameter l, of 5% for parameter m, and of 18% for the resulting dispersion is achieved. The higher deviation for the resulting dispersion compared to the calculated parameters can be explained by the fact that for the determination of the parameters l and m, an averaged dispersion curve over the mixing time is established based on the data points. Consequently, the parameters l and m are already based on averaged data, whereas the comparison of the resulting dispersion compares the actual measured data with the calculated data. For the resulting dispersion, the deviation between the values based on measured data and calculated with the resulting function from SR exceeds the required deviation of 15%. In the case of SR, the results represent mathematical equations of different complexity, whereby the complexity describes the number of operators and variables of one equation [15]. However, further increasing the complexity of the equation determined by SR does not improve the accuracy of the prediction. Analogously to the incorporation, an improvement in the prediction above a dispersion of 80% to an average deviation of 8% is achieved. A possible reason might be that the carbon black is not sufficiently in corporated at the beginning of the mixing process. This leads to the assumption of a better dispersion, since less agglomerates are present due to the lower amount of carbon black [26]. To improve the calculation of the dispersion degree in further investigations, *Leigh-Dugmore* developed a method that calculates the percentage of dispersed agglomerates in relation to the amount of filler used [27]. In order to take the rubber included in the agglomerate into account, a factor empirically developed by *Medalia* is added, which gives the average amount of carbon black per agglomerate [28].

5.3 | Distribution

As last model for predicting mixing quality, the distribution curve for carbon black is determined. The calculation assumes that the distribution can be described by the distribution of carbon black agglomerates. For this reason, the standard deviation of the dispersion is divided by the mean value. A smaller value represents a better distribution. Similar to the description of the dispersion, the distribution curve is derived from the measured data. The superordinate function for the distribution curve can be taken from Equation (21).

$$Distribution = o * R^{-p} \tag{21}$$

The dependence of the parameters o and p on the material and process parameters is determined using SR (Equation (22) and (23)).

$$o = d * (((FF - T_M)/((FF * 0.64) - E)) + 64.15) \tag{22}$$

$$p = ((\delta - 19.47) * ((4.43/\delta) - (7.89/T_M))) + 2.9 \tag{23}$$

Parameter o indicates a relationship to the material parameters: δ and ethylene content as well as to the process parameters fill factor and rotor temperature. To calculate the parameter p δ and the mixing chamber temperature are taken into account. To validate the calculated parameters, Figure 9 shows the comparison between the parameters obtained from the mixing process and the calculated parameters. In addition, the measured distribution is shown in comparison to the calculated distribution, which results from the parameters calculated using SR.

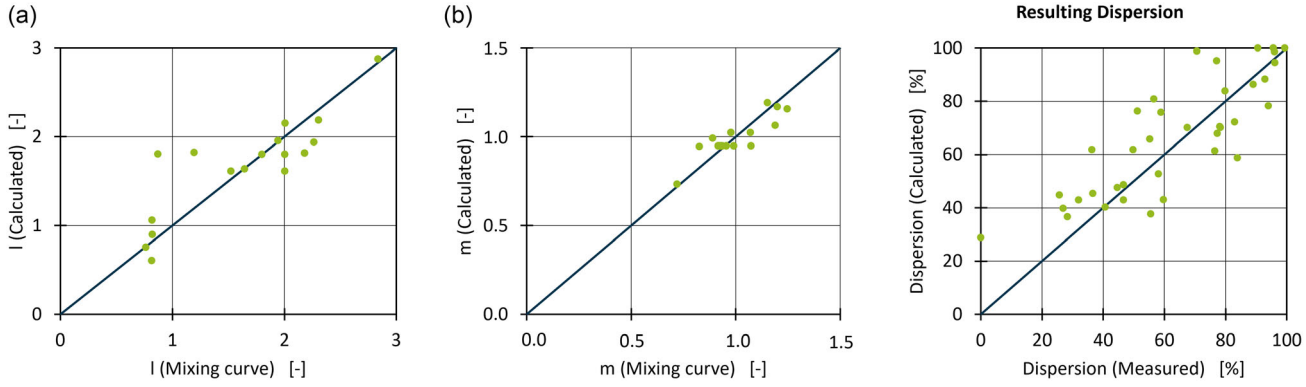


FIGURE 8 | Comparison of the parameters and the resulting curve for the dispersion based on the mixing curves and the calculated parameters.

15272648, 0, Downloaded from https://advanced.onlinelibrary.wiley.com/doi/10.1002/adem.202503201 by Universitatsbibliothek RWTH Aachen University, Wiley Online Library on [29/05/2026]. See the Terms and Conditions (https://onlinelibrary.wiley.com/terms-and-conditions) on Wiley Online Library for rules of use; OA articles are governed by the applicable Creative Commons License

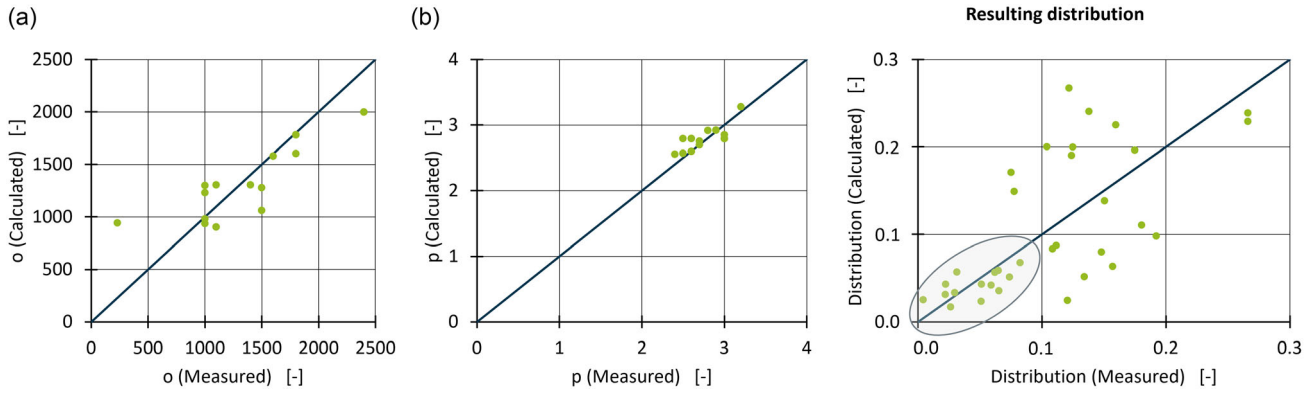


FIGURE 9 | Comparison of the parameters and the resulting curve for the distribution based on the mixing curves and the parameters calculated with SR.

An average deviation of 14% for parameter o between the measured and calculated data points and of 2% for parameter p is achieved. For the total distribution the average deviation results in 63%. Using only values below 0.1 the average deviation decreases by 20%. Similar to the calculation of the dispersion, the lower accuracy of the prediction of the distribution curve compared to the parameters can be explained due to the fact that the parameters o and p are already determined from the average distribution, resulting in a lower correlation with the measured distribution for the individual data points. In addition, the reduced amount of incorporated carbon black at the beginning of the mixing process results in a lower standard deviation and thus a better calculated distribution. As a result, the distribution is assumed to be higher compared to the actual distribution.

6 | Optimization of the Mixing Time and Energy Input

The aim of optimization is to identify the combination of process parameters and polymer type which results in a reduction of mixing time and energy input. In order to determine the mixing time of a mixing process, the models for incorporation, dispersion, and distribution are applied. In this context, it is defined that incorporation and dispersion values of at least 95% are required. To define a value indicating sufficient distribution, Figure 10 shows the distribution values over the mixing time using Keltan 6950C, a rotor and mixing chamber temperature of 40°C, a rotor speed of 45, and a fill factor of 70%.

For the compounds analyzed, it was therefore specified that a distribution value below 0.05 is required to ensure homogeneity. As previously explained, the distribution cannot be predicted with a high degree of accuracy based on the available data. However, to determine the point at which the compound can be discharged from the mixing chamber, the selected optimal distribution serves primarily as a guideline for the completion of the mixing process and not as a fully predictive model. Furthermore, an incorporation time between 10 and 100 s should be achieved to ensure an optimum fill factor of the mixing chamber. The energy input is calculated using the three models for torque (T_1, T_2, T_3). For the optimization of the analyzed mixing process, the polymer and process parameters will be varied in the applied models.

In order to obtain feasible values for the machine equipment and the developed models, the process and material parameters will be limited to the value ranges listed in Table 4.

The optimization was performed with an evolutionary algorithm as described in Chapter 2.2.1 and implemented with the "Distributed Evolutionary Algorithms" (DEAP) framework in python [29]. For the optimization, the algorithm with the function" deap.algorithms.eaMuPlusLambda" was implemented [30].

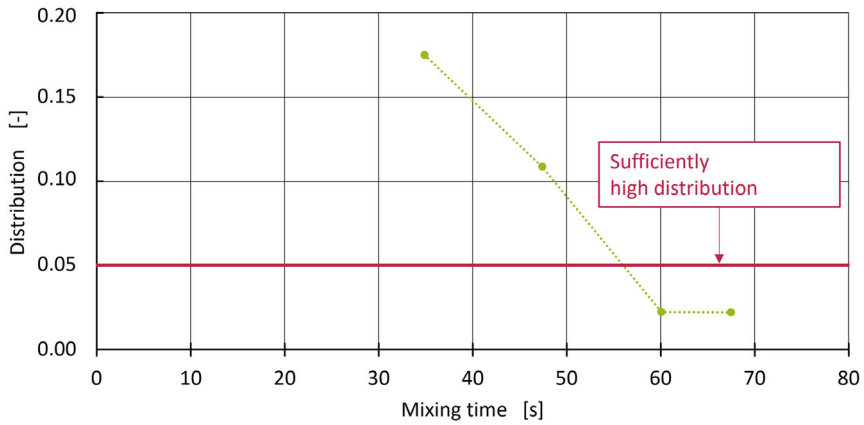


FIGURE 10 | Distribution over the mixing time using Keltan 6950C, a rotor and mixing chamber temperature of 40°C, a rotor speed of 45, and a fill factor of 70% to define the required distribution value.

15272648, 0, Downloaded from https://advanced.onlinelibrary.wiley.com/doi/10.1002/adem.202503201 by Universitatsbibliothek RWTH Aachen University, Wiley Online Library on [29/05/2026]. See the Terms and Conditions (https://onlinelibrary.wiley.com/terms-and-conditions) on Wiley Online Library for rules of use; OA articles are governed by the applicable Creative Commons License

TABLE 4 | Limitation of process parameters for the optimization.

Process parameter	value range
Temperature rotor [°C]	30–60
Temperature mixing chamber [°C]	30–60
Rotor speed [min^{-1}]	30–60
Fill factor [%]	65–75
Polymer parameter	**value range**
δ [rad/s]	14–25
Δδ [rad/s]	15–40
Ethylene-content [wt.-%]	40–60

For each of the 20 generations, a population of 10 individuals is generated, each representing one mixing process.

6.1 | Results of Optimization and Discussion

Based on the optimization described, the shortest mixing time in combination with the lowest energy input is achieved using the EPDM polymer type Keltan 2750 and a filling factor of 75%, a rotor speed of 35 min^{-1}, a rotor temperature of 30°C, and a mixing chamber temperature of 47°C. This specific parameter combination was not included among the experimental runs used to establish the models and therefore provides an independent test case.

To validate both the models and the optimization result, a dedicated follow-up experiment was carried out under these optimized conditions in the internal mixer. A compound was produced using the optimized settings, and the resulting mixing curves were recorded. Subsequently, the measured mixing curves were compared with the curves calculated from the models (Figure 11).

With regard to the mixing curves, the measured and calculated mixing curves display a good correlation in terms of the ram path, particularly with regard to the time required to reach the end position of the ram. The calculated mixing curve reaches the end position 1.8 s in advance of the measured mixing curve, which corresponds to a deviation of 7%. Consequently, the model for the ram position can be considered to be sufficiently accurate.

Referring to the torque curve, deviations can be observed. In the first mixing phase until reaching the end position of the ram, there is an average deviation of 17% between the measured and calculated torque curves. Furthermore, when the end position of the ram is reached, the measured mixing curve achieves a maximum torque, which is 22% higher compared to the calculated mixing curve. One possible reason could be the insufficiently accurate prediction of incorporation at the beginning of the mixing process, as a higher amount of incorporated carbon black leads to an increase in compound viscosity and thus to higher torque [31]. An integration of the incorporation progress should therefore be included in following models. The second mixing phase for calculating the torque curve is bounded by the two torque maxima. It should be noted that the calculated torque curve remains underneath the measured torque curve, resulting in an average deviation of 24%. In addition, the calculated torque curve reaches the second torque maximum approximately 12 s after the measured torque curve, which corresponds to a deviation of 20%. It is assumed that the differences in the torque curve can be related to the higher actual amount of incorporated carbon black than assumed with the model for the torque in the second mixing phase [31]. Furthermore, the higher torque and the related higher shear stress can lead to improved dispersion [32]. As a result, the second torque maximum is reached earlier, as this can be associated with the completion of dispersion. However, regarding the absolute height of the second torque maximum, a sufficiently accurate prediction is achieved with a deviation of approximately 9%. Considering the third mixing phase, where the torque decreases due to a reduction in viscosity, a mean deviation of 9% can be observed between the measured and calculated mixing curves. It is therefore considered that the second torque maximum is reached at the same time. As a result, a sufficiently high accuracy can be achieved for the third mixing phase. Overall, the models developed can be used to describe the ram position and torque in the third mixing phase with sufficient accuracy. With regard to the torque in the third mixing phase, this mixing phase is characterized by the fact that the fillers are already completely incorporated and dispersed. Thus, adding parameters to describe the dependence of the models on the progress of incorporation and dispersion during the first two mixing phases is recommended.

The comparison shows that the models reproduce the overall shape and main trends of the mixing curves, but noticeable

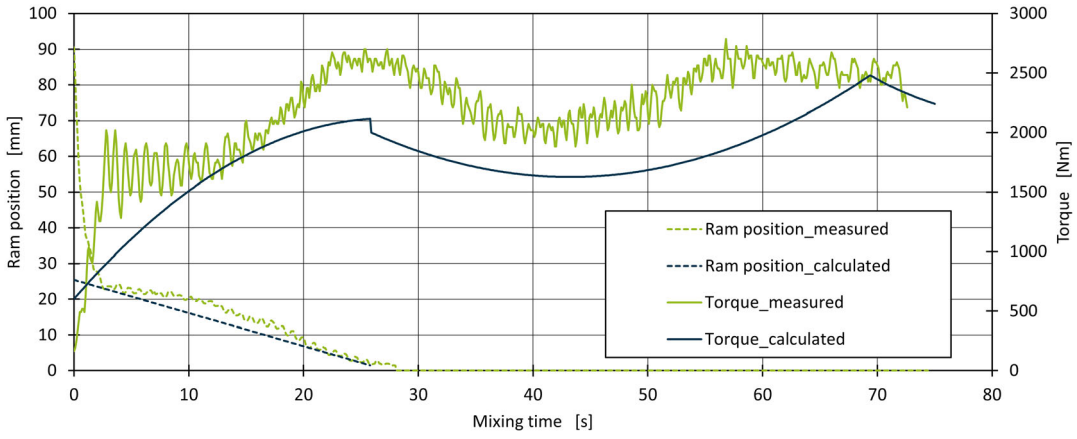


FIGURE 11 | Comparison of the calculated and measured mixing curves after optimization.

15272648, 0, Downloaded from https://advanced.onlinelibrary.wiley.com/doi/10.1002/adem.202503201 by Universitatsbibliothek RWTH Aachen University, Wiley Online Library on [29/05/2026]. See the Terms and Conditions (https://onlinelibrary.wiley.com/terms-and-conditions) on Wiley Online Library for rules of use; OA articles are governed by the applicable Creative Commons License

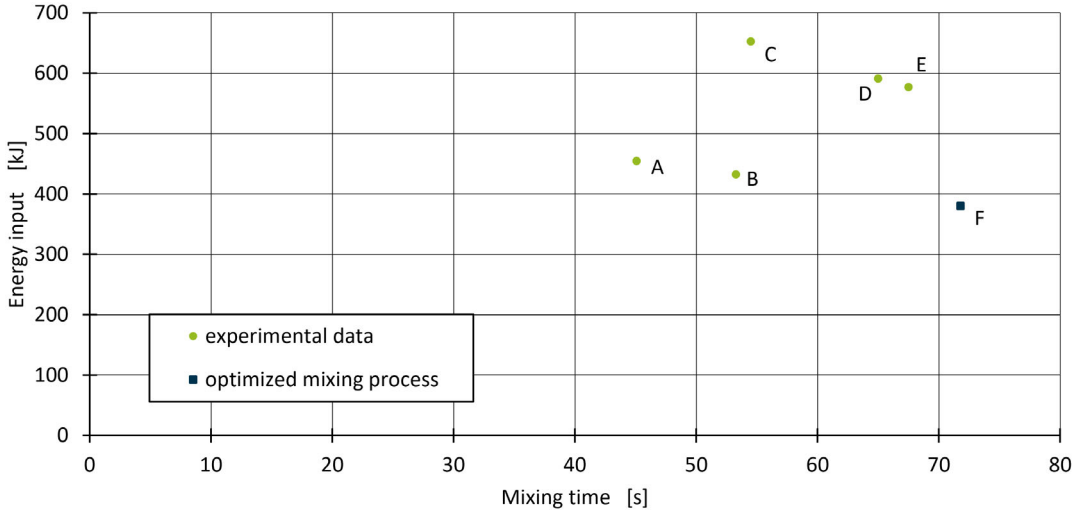


FIGURE 12 | Comparison of the optimized compound with the experimental data used for the development of the models in terms of mixing time and energy input.

quantitative deviations occur in certain regions. This independent experiment thus provides an external validation in the sense that the dominant process behavior is captured, while at the same time highlighting the limited quantitative accuracy of the models, which is consistent with the small size and restricted variability of the underlying dataset.

The deviations in torque prediction in the first and second mixing phases show a systematic trend. For the validation mixing process, the model underestimates the torque in these phases. As a consequence, the actual torque and thus the shear stresses during the mixing process are higher than those calculated by the model. Since dispersion kinetics in internal mixing are primarily driven by shear stress, this implies that the model is conservative with respect to mixing quality. For given operating conditions and a given mixing time, the actual process is expected to reach the target values earlier than predicted by the model. With regard to the objective function, the optimization is based on energy consumption over the entire mixing cycle. Underestimating the torque therefore, leads to an underestimation of the specific energy consumption for the validation mixture. This deviation affects the absolute values of energy consumption and may also may shift the exact location of the optimum. The optimized operating point determined in this study should therefore be interpreted as an experimentally confirmed, energy-efficient solution rather than as the sole global optimum that would be achieved with a perfectly accurate model. The second aim is to validate whether the selected optimization strategy can reduce mixing time and energy input. For this reason, Figure 12 shows the mixing time and energy input of the compounds produced for the development of the models (green) and the optimized mixture (blue). To compare mixing times and energy consumption, experimental data were used for all mixing processes. This refers to both the data sets used for modeling and the optimized mixing process. The corresponding process parameters can be obtained from Table 5. In this context, only compounds with sufficient mixing quality (in corporation, dispersion >95%, distribution <0.05) are considered.

A comparison between point C and the optimized mixture shows a 40% reduction in energy consumption and a 35% reduction compared to reference point E. However, a longer mixing time is required to reach the required mixing quality. If dispersion and distribution are determined from the surface topography for the optimized operating conditions, a dispersion degree of 98% and a distribution value of 0.01 are obtained. This confirms that the mixing quality achieved under the optimized conditions is sufficiently high, despite the reduced specific energy input. In addition, the end of the mixing process is defined by the attainment of the required mixing quality. The values determined for dispersion and distribution therefore indicate that a shorter mixing time may still be suitable while maintaining the required mixing quality.

TABLE 5 | Parameters for the comparison.

	EPDM-polymer-type	Temperature Rotor, °C	Temperature Mixing chamber, °C	Rotor speed, min^{-1}	Fill factor, %
A	Keltan 2750	40	40	45	70
B	Keltan 6950 C	80	30	45	70
C	Keltan 6950 C	40	40	60	70
D	Keltan 6950 C	30	30	45	70
E	Keltan 6950 C	40	40	40	70
F	Keltan 2750	30	47	35	75

15272648, 0, Downloaded from https://advanced.onlinelibrary.wiley.com/doi/10.1002/adem.202503201 by Universitatsbibliothek RWTH Aachen University, Wiley Online Library on [29/05/2026]. See the Terms and Conditions (https://onlinelibrary.wiley.com/terms-and-conditions) on Wiley Online Library for rules of use; OA articles are governed by the applicable Creative Commons License

7 | Conclusion and Outlook

SR was used to describe the mixing process as a function of the process parameters fill factor, rotor speed, mixing chamber and rotor temperature control, and the type of EPDM polymer used. In total, seven models were developed describing the mixing curves for the ram position and torque as well as the mixing quality based on the development of incorporation, dispersion, and distribution. For all models, a superior function was first determined, which is used to obtain parameters which are subsequently determined as a function of the specified process and polymer parameters. For the mixing curves of the ram position and torque, models with sufficient accuracy and an average deviation of less than 15% could be generated. However, a reduced accuracy of less than 15% was observed for the models describing the mixing quality. Reasons for this include an insufficient number of tests and the dependence of dispersion and distribution on incorporation, which results in higher measured values, especially in the range of lower amounts of incorporated carbon black. An improvement in the accuracy for the prediction of incorporation and dispersion can be observed, with an average deviation of less than 15% using values above 80% incorporated or dispersed carbon black. Thus, the determined function is sufficiently accurate for determining the time where 95% of the carbon black is incorporated and dispersed and the mixing quality is thus sufficiently accurate. With regard to distribution, it was not possible to achieve a sufficiently accurate prediction. Therefore, further tests should be carried out to enable a prediction of the distribution.

Based on the developed models, an optimization was carried out using evolutionary algorithms. The aim was to reduce the mixing time and energy input. In addition, 95% of the carbon black had to be incorporated and dispersed, and the distribution should be less than 0.05. Overall, it was observed that a reduction in energy input could be achieved by increasing the mixing time. In order to achieve a reduction in mixing time and energy input, a more complex process design could be applied, for example, by the variation of rotor speed over mixing time. In addition, the developed models were validated using the optimized mixture in terms of mixing time and energy input. For this purpose, the mixture was produced in the internal mixer similar to the compounds used for developing the models, and measured afterwards. Overall, the results indicate that the ram path can be predicted with sufficient accuracy, achieving a deviation of 7% between the measured and calculated incorporation time. With regard to torque, an average deviation of up to 24% was observed in the individual phases. It is assumed that these deviations are caused by a higher proportion of incorporated carbon black.

Therefore, in the following models, the development of the mixing quality should be included in the description of the mixing curves, as the amount of carbon black influences the viscosity and thus the torque. With regard to the material parameters, previously only different types of EPDM polymer were taken into account. Further investigations should therefore consider different types of carbon black and the amount of carbon black used. Previous studies have already demonstrated the influence of different types of carbon black on the mixing process. For example, a higher degree of carbon black structure results in a longer ram down time and a faster dispersion rate, which correlates with higher power input [33]. These results have not yet been integrated into models. In addition, the influence of other mixer sizes should be investigated. Following the extension and optimization of the models, these are to be integrated into a database in order to be able to provide a suggestion for an optimized mixing instructions based on the recipe and the given plant technology.

Acknowledgments

The investigations set out in this report received financial support from the German Federal Ministry of Research, Technology and Space (No. 13XP5196G), to whom we extend our thanks.

Open Access funding enabled and organized by Projekt DEAL.

Funding

This study was supported by Bundesministerium für Forschung und Technologie (13XP5196G).

Conflicts of Interest

The authors declare no conflicts of interest.

Data Availability Statement

The data that support the findings of this study are available from the corresponding author.

References

1. A. Limper, A. Holzner, F. Röthemeyer, F. Sommer, *Kautschuktechnologie: Werkstoffe-Verarbeitung-Produkte : Band, neu bearbeitete und erweiterte auflage edition 1* (Hanser eLibrary. Hanser, 2025,

2. E. Haberstroh, *Neuartige Methode zur Optimierung Des Mischprozesses Im Kautschuk- Innenmischer* (Abschlussbericht, 2016).

3. T. A. Osswald, "Verarbeitungsprozesse mit Modellen beschrieben," *Kunststoffe* 93, no. 10 (2003): 130.

4. A. Limper, *Mixing of Rubber Compounds* (Hanser Publishers and Hanser Publications, 2012).

5. C. Hopmann and U. Epple, "Erhöhung der Energieeffizienz Bei der Kautschukverarbeitung Durch Eine Mischzeitreduktion Auf Basis Datengeriebener, Mathematischer Modelle," *Abschlussbericht* (2019).

6. C. Hopmann, M. Kostka, A. Limper, and M. Facklam, *Gummi Fasern Kautschuk GAK* 74 (2021): 1–2.

7. P. R. van Buskirk, S. B. Turetzky, and P. F. Gunberg, "Practical Parameters for Mixing," *Rubber Chemistry and Technology* 48, no. 4 (1975): 577.

8. A. Bardehle, A. Limper, L. Leuchtenberger-Engel, C. Hopmann, M. Rinker, and L. Hermeling, "Modelling of the Filler Incorporation during the Rubber Mixing Process using EPDM," *Kautschuk, Gummi, Kunststoffe: KGK* 78, no. 4 (2025): 42–49.

9. M. Bratina, Z. Susteric, B. Ster, U. Lotric, and A. Dobnikar, "Predictive Control of Rubber Mixing Process Based on Neural Network Models," *Kautschuk Gummi Kunststoffe KGK* 62, no. 7 (2009): 378–382.

10. P. Ryzko, *Dissertation* (RWTH Aachen, 2001).

11. C. Hopmann, M. Kostka, L. Seifert, A. Limper, and M. Schön, *Kautschuk Gummi Kunststoffe KGK* 76, no. 5 (2023): 72.

12. C. Hopmann, A. Bardehle, A. Limper, and L. Leuchtenberger-Engel, *Kautschuk Herbst Kolloquium KHK* (2024).

13. T. Avalosse, B. Alsteens, and V. Legat, "Rotor Shape Design by Numerical Simulation: A New Way to Improve Dispersive and Distributive Mixing in Batch Mixers," *Elastomery* 9 (2005): 16.

15272648, 0, Downloaded from https://advanced.onlinelibrary.wiley.com/doi/10.1002/adem.202503201 by Universitatsbibliothek RWTH Aachen University, Wiley Online Library on [29/05/2026]. See the Terms and Conditions (https://onlinelibrary.wiley.com/terms-and-conditions) on Wiley Online Library for rules of use; OA articles are governed by the applicable Creative Commons License

14. L. Guo, C. S. Wang, and H. G. Bian, "FEA of Flow Fluid of Six-Wing Synchronous Varying Clearance Rotor," *Key Engineering Materials* 561 (2013): 59.

15. R. Hollstein, *Optimierungsmethoden: Einführung in Die Klassischen, Naturanalogen Und Neuronalen Optimierungen* (Springer Vieweg, Wiesbaden and Heidelberg, 2023).

16. L. Hermeling, Ph.D. Thesis (Universität Siegen, 2022).

17. D. Ferrari, V. Guidetti, Y. Wang, and V. Curcin, "AMIA Annual Symposium Proceedings," AMIA Symposium (2022), 442, 2022.

18. D. Ferrari, "Multi-Objective Symbolic Regression for Data-Driven Scoring System Management," in 2022 IEEE International Conference on Data Mining (ICDM) (2024).

19. R. Hornig and J. Kielmann, "Oscillation Rheology vs. High-Pressure Capillary Rheometry," *Gummi Fasern Kunststoffe* 11 (2014): 708.

20. T. Sajjayanukul, P. Saeoui, and C. Sirisinha, "Experimental Analysis of Viscoelastic Properties in Carbon Black-Filled Natural Rubber Compounds," *Journal of Applied Polymer Science* 97, no. 6 (2005): 2197.

21. J. S. Dick and H. Pawloski, *Practical Rubber Rheology and Dynamic Properties* (Hanser).

22. P. W. Meijers, L. R. Maag, H. J. Beelen, and P. M. van de Ven, "Advances in EPDM Technology: Structure Determination as a Key to Improved Product Performance and Consistency," *KGK Kautschuk Gummi Kunststoffe* 52, no. 10 (1999): 663.

23. M. van Duin, H. Dikland, T. Fŕuh, T. Groß, C. Haßmann, N. Sary, and R. Schmidt, *Handbook of Synthetic Rubber* (ARLANXEO Deutschland GmbH, 2020).

24. D24 Committee, Test Methods for Carbon Blackdispersion in Rubber.

25. J. J. Brennan, T. E. Jermyn, and B. B. Boonstra, "Carbon Black–Polymer Interaction: A Measure of Reinforcement," *Journal of Applied Polymer Science* 8, no.6 (1964): 2687.

26. J. R. Campanelli, C. Gurer, T. L. Rose, and J. E. Varner, "Dispersion, Temperature and Torque Models for an Internal Mixer," *Polymer Engineering & Science* 44, no.7 (2004): 1247.

27. C. H. Leigh-Dugmore, "Measurement of Dispersion in Black-Loaded Rubber," *Rubber Chemistry and Technology* 29, no. 4 (1956): 1303.

28. A. I. Medalia, "Dispersion of Carbon Black in Rubber: Revised Calculation Procedure," *Rubber Chemistry and Technology* 34 (1961): 1134.

29. NN, Deap documentation, https://deap.readthedocs.io/en/master/.

30. F. De Rainvill, et al., Deap, https://github.com/DEAP/deap.

31. N. P. Cheremisinoff and P. N. Cheremisinoff, *Handbook of Applied Polymer Processing Technology* (CRC Press, 1996).

32. G. Focht, Ph.D. Thesis, (Universität Siegen, 2018).

33. C. Hopmann, A. Bardehle, M. Kostka, A. Limper, L. Leuchtenberger, and M. Schön, *Kautschuk Gummi Kunststoffe KGK* 77, no. 3 (2023): 56.

Supporting Information

The supporting information data are available from the corresponding author upon reasonable request.

15272648, 0, Downloaded from https://advanced.onlinelibrary.wiley.com/doi/10.1002/adem.202503201 by Universitatsbibliothek RWTH Aachen University, Wiley Online Library on [29/05/2026]. See the Terms and Conditions (https://onlinelibrary.wiley.com/terms-and-conditions) on Wiley Online Library for rules of use; OA articles are governed by the applicable Creative Commons License